

# Mechanism of Retinal Schiff Base Formation and Hydrolysis in Relation to Visual Pigment Photolysis and Regeneration: Resonance Raman Spectroscopy of a Tetrahedral Carbinolamine Intermediate and Oxygen-18 Labeling of Retinal at the Metarhodopsin Stage in Photoreceptor Membranes

Alan Cooper,\* Sheila F. Dixon, Margaret A. Nutley, and Jenifer L. Robb

Contribution from the Department of Chemistry, Glasgow University, Glasgow G12 8QQ, Scotland, U.K. Received October 15, 1986

**Abstract:** The mechanism of formation and hydrolysis of *N*-retinylidene-*n*-butylamine, as a model of the rhodopsin chromophore, has been investigated by a study of the kinetic and equilibrium properties in aqueous anionic, cationic, and neutral detergent micelle systems. The pH dependence of steady-state formation and hydrolysis rate constants is consistent with the classical imine reaction mechanism involving tetrahedral carbinolamine intermediates. Kinetic transients consistent with such intermediates can be seen using rapid stopped-flow techniques. Hydrolysis rates in neutral detergent micelles exhibit general base catalysis, and there are pronounced detergent-specific effects which can be qualitatively interpreted in terms of ionic effects on Schiff base  $pK_a$  and micellar hydrogen ion activities. This suggests a rational explanation for the anomalous  $pK_a$  and thermodynamic stability of visual pigment chromophores under physiological conditions. The tetrahedral intermediate has been observed directly at room temperature by continuous-flow, pH-jump resonance Raman spectroscopy, and the spectrum of this transient species shows remarkable similarity with the previously reported Raman spectrum of the metarhodopsin II intermediate of bovine rhodopsin photolysis. Isotope-labeling experiments on bovine photoreceptor membranes exposed to oxygen-18 enriched water during bleaching show incorporation of  $^{18}O$  at the retinal aldehyde site during the metarhodopsin I  $\rightarrow$  II transition. These observations support the hypothesis that the vertebrate Meta I  $\rightarrow$  Meta II transition involves hydrolytic attack by water on the retinyl-lysine Schiff base linkage of the rhodopsin chromophore.

Visual pigment rhodopsins and related proteins from various organisms are characterized by the presence of the retinal chromophore, attached via a Schiff base (imine) linkage to a specific lysine side chain.<sup>1</sup> In vertebrate rhodopsins, at least, this linkage is hydrolyzed at some stage during the visual photochemical cycle (after *cis*-*trans* photoisomerization) and must be re-formed (with 11-*cis*-retinal) during regeneration. Neither the precise stage at which this hydrolysis occurs nor, indeed, the mechanism of Schiff base formation and hydrolysis in the protein active site environment is known. We report here on a series of experiments designed to clarify the situation. Firstly, using conventional equilibrium and kinetic techniques, we examine the formation and hydrolysis of a model retinal Schiff base in different detergent micelle environments in relation to the standard tetrahedral carbinolamine intermediate mechanism of imine chemistry.<sup>2</sup> The presence of this intermediate is demonstrated by stopped-flow kinetic measurements and its resonance Raman spectrum obtained under continuous flow conditions. Finally, using isotope-labeling techniques, we examine the possible onset of Schiff base hydrolysis during the metarhodopsin stage of photolysis in bovine photoreceptor membranes.

## Experimental Section

**Model Compound Equilibrium and Kinetics.** *all-trans*-Retinal (vitamin A aldehyde, retinaldehyde, from Fluka or Sigma) was used without

further purification. Mass spectrometry and HPLC analysis showed no detectable impurities other than traces of other geometric isomers. Detergents used include: Emulphogene BC-720 (a commercial poly(oxyethylene-10-tridecyl ether) preparation from GAF), Ammonyx-LO (primarily lauryl dimethylamine oxide, from Onyx Corp.), sodium dodecyl sulfate (SDS, from BDH Ltd.), and dodecyltrimethylammonium bromide (DTAB, from Sigma). *n*-Butylamine was redistilled before use, and all other reagents were of appropriate analytical grade. Glass-distilled water was used throughout, and all manipulations involving retinal were done under argon in the dark or dim light conditions.

Retinal solutions for kinetic and equilibrium experiments were made up fresh daily by first dissolving the solid in a small quantity of ethanol, followed by rapid dispersal in a large volume of the appropriate detergent buffer (final EtOH concentration less than 1%). Stock solutions of the model Schiff base, *N*-retinylidene-*n*-butylamine, were prepared by addition of retinal to a large excess of 10 mM *n*-butylamine in ethanol or unbuffered aqueous detergent. Incubation at room temperature for 30 min was sufficient for complete reaction. All experiments were performed at 20 °C. Buffer concentrations were generally 0.1 M, except in the case of SDS where poor solubility limited buffer concentrations to 0.02 M. Detergent concentrations used were well above critical micelle concentrations: 2% v/v (Ammonyx, Emulphogene), 25 mM (DTAB), and 12.5 mM (SDS). Spectral changes in the 300-550-nm range were observed using Pye-Unicam SP-1800 or SP-200 spectrophotometers fitted with thermostated cell holders.

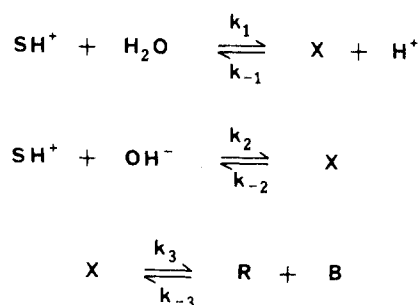
Dissociation constants ( $K_{obsd}$ ) for the retinal-butylamine reaction were determined in the pH range 7-13 using phosphate, borate, or NaOH/NaCl buffers, as appropriate. Retinal in detergent buffer was mixed, under argon, in a series of stoppered volumetric flasks with appropriate volumes of *n*-butylamine in the same buffer mixture, to give a final retinal concentration of about  $10^{-5}$  M and butylamine concentrations in the range 0.02 mM to 1 M. After incubation for 2-4 h at 20 °C spectra were taken to determine the extent of reaction. The pH of each mixture was checked before and after incubation. Longer reaction times gave identical results, as did trial experiments in which equilibrium was approached from the opposite direction by pH and concentration adjustment of solutions of the preformed Schiff base. Data were analyzed by a linear least-squares Benesi-Hildebrand method<sup>3</sup> using absorbances at a minimum of two different wavelengths for each sample.

(1) For background see: (a) Wald, G. *Science* **1968**, *162*, 230. (b) Knowles, A.; Dartnall, H. J. A. *The Eye*, 2nd ed.; Academic Press: New York, 1977; Vol. 2B. (c) Honig, B. *Annu. Rev. Phys. Chem.* **1978**, *29*, 31. (d) Birge, R. R. *Annu. Rev. Biophys. Bioeng.* **1981**, *10*, 315. (e) Balogh-Nair, V.; Nakanishi, K. In *New Comprehensive Biochemistry*, Vol. 3, *Stereochemistry*; Tamm, Ch., Ed.; Elsevier Biomedical Press: Amsterdam, 1982; p 283. (f) Findlay, J. B. C.; Pappin, D. J. C. *Biochem. J.* **1986**, *238*, 625. For reviews of photolysis intermediates, see: (g) Applebury, M. L. *Vision Res.* **1984**, *24*, 1445. (h) Ostroff, S. E. *Biochim. Biophys. Acta* **1977**, *463*, 91. (i) Birge, R. R. In *Biological Events Probed by Ultrafast Laser Spectroscopy*; Academic Press: New York, 1982; p 299.

(2) (a) Jencks, W. P. *Catalysis in Chemistry and Enzymology*; McGraw-Hill: New York, 1969. (b) Cordes, E. H.; Jencks, W. P. *J. Am. Chem. Soc.* **1963**, *85*, 2843. (c) Jencks, W. P. *Ibid.* **1959**, *81*, 475.

(3) Benesi, H. A.; Hildebrand, J. H. *J. Am. Chem. Soc.* **1949**, *71*, 2703.

Scheme I



Steady-state rates of Schiff base formation and hydrolysis were obtained from absorbance changes, again at at least two wavelengths, after mixing retinal or the Schiff base with the relevant detergent buffer mixture. Variation of the butylamine content verified that formation rates were first order in amine concentration. Absorbance changes were recorded either at fixed wavelengths or, for slower reactions, by repetitive spectral scans, and the pH of each reaction mixture was determined at the end of each kinetic run using a sodium ion correction at high pH if appropriate. Pseudo-first-order rate constants ( $k_{\text{form}}$  or  $k_{\text{hydro}}$ ) were obtained by least-squares analysis according to the appropriate first-order rate expression, and formation rate constants were corrected for hydrolysis in the reverse direction when necessary. This latter correction is only significant at the lower pH limit and never amounted to more than 10% of the whole. A limited examination of possible solvent isotope effects was undertaken for hydrolysis in Ammonyx with D<sub>2</sub>O (99.8%, Fluorochem, pD 4.0).

General base catalysis of the hydrolysis reaction in Emulphogene or Ammonyx micelles was investigated in the pH range 4–7 by use of various different buffers over a concentration range of 0.01 to 0.2 M. Higher concentrations could not be used because of problems with solubility of the detergents. Control experiments with added NaCl showed that ionic strength had no significant effect on hydrolysis rates in this pH range.

Transient kinetics were studied using an Applied Photophysics stopped-flow kinetic spectrophotometer, interfaced to an Apple II microcomputer giving nonlinear, programmable time-base data acquisition. The effective dead-time of this apparatus is about 8 ms, and the nonlinear time-base allows data in the time range from about 10 ms to 12 min to be sampled in a single run. Rapid formation or hydrolysis reactions were initiated by pH-jump or reagent mixing, as appropriate, and the kinetic behavior was analyzed by a multiexponential fitting procedure (DISCRETE) kindly provided by Dr. Provencher.<sup>4</sup>

The hydrogen ion titration behavior of the model Schiff base in different detergents was obtained from the absorbance changes associated with the protonation-induced red shift of the retinyl chromophore during pH-jump experiments. Absorbances at 360 and 440 nm, extrapolated to zero time, were obtained from the initial phases of stopped-flow measurements (<100 ms) and were confirmed, in the slower hydrolysis ranges, by manual mixing techniques. Data were analyzed from the pH dependence of the quantity:

$$[\text{SH}^+]/[\text{S}] = (A_{\text{H}} - A)/(A - A_{\text{L}})$$

where  $A_{\text{H}}$  and  $A_{\text{L}}$  are the initial absorbances at high and low pH extremes,  $A$  is the initial absorbance after pH-jump, and  $\text{SH}^+$  and  $\text{S}$  are the protonated and unprotonated Schiff base, respectively.

Defining the acid dissociation constant of the Schiff base:

$$K_{\text{SH}} = [\text{S}]a_{\text{H}}/[\text{SH}^+]$$

where  $a_{\text{H}}$  is the hydrogen ion activity in the micelle, shows that, for simple titration behavior, a plot of  $\log [\text{S}]/[\text{SH}^+]$  vs.  $\text{p}a_{\text{H}}$  should be linear, with slope unity and an intercept of  $\text{p}K_{\text{SH}}$  on the  $\text{p}a_{\text{H}}$  axis. To relate the micellar hydrogen ion activity to the measured bulk pH, we use the empirical relation:

$$\text{p}a_{\text{H}} = n(\text{pH}) - p\phi \quad (1)$$

where  $p\phi$  and  $n$  represent any apparent pH shift and nonideality at the micelle, respectively. ( $n = 1$  for ideal titration behavior.) We arbitrarily take  $p\phi = 0$  for the neutral detergent, Emulphogene. The midpoint pH of the titration is given, in these terms, by:

$$\text{pH}_{\text{mid}} = (\text{p}K_{\text{SH}} + p\phi)/n$$

**Reaction Mechanism: Equilibrium and Rate Expressions.** We assume the standard<sup>2</sup> imine mechanism (Scheme I) in which retinal Schiff base hydrolysis and formation share a common tetrahedral carbinolamine intermediate (X). X is formed solely by attack of water or hydroxide on the protonated imine ( $\text{SH}^+$ ), or by reaction of unprotonated amine (B) on the aldehydic retinal (R). Assuming that all retinyl species are confined to the micellar phase, whereas the much more soluble free butylamine resides in the aqueous phase, we can define the following acid dissociation constants for the amine and imine, respectively:

$$K_{\text{BH}} = [\text{B}][\text{H}^+]/[\text{BH}^+] \quad K_{\text{SH}} = [\text{S}]a_{\text{H}}/[\text{SH}^+]$$

where  $[\text{H}^+]$  is the hydrogen ion concentration (strictly activity) in the bulk aqueous phase (as measured by the pH electrode) and  $a_{\text{H}}$  is the hydrogen ion activity in the micellar phase estimated from the Schiff base titrations in the appropriate detergents as described above.

The overall observed equilibrium constant for the reaction ( $K_{\text{obsd}}$ ) may be written:

$$\begin{aligned}
 K_{\text{obsd}} &= [\text{B}]_{\text{tot}}[\text{R}]/[\text{S}]_{\text{tot}} \\
 &= K_0(1 + [\text{H}^+]/K_{\text{BH}})/(1 + a_{\text{H}}/K_{\text{SH}}) \quad (2)
 \end{aligned}$$

where  $K_0 = [\text{R}][\text{B}]/[\text{S}]$  is the dissociation constant at the high pH limit. Application of detailed balance gives several useful relations between the equilibrium and rate constants:

$$k_1k_{-2}/k_{-1}k_2 = a_{\text{H}}a_{\text{OH}} = K_{\text{w}}$$

$$K_0 = k_2k_3K_{\text{w}}/k_{-2}k_{-3}K_{\text{SH}} = k_1k_3/k_{-1}k_{-3}K_{\text{SH}}$$

Following established procedures,<sup>2,5</sup> steady-state pseudo-first-order and second-order observed rate constants for hydrolysis and formation, respectively, may be written:

$$\begin{aligned}
 k_{\text{hydro}} &= \frac{k_3}{(a_{\text{H}} + K_{\text{SH}})} \left( \frac{k_1a_{\text{H}} + k_2K_{\text{w}}}{k_3 + k_{-2} + k_{-1}a_{\text{H}}} \right) \\
 k_{\text{form}} &= \frac{k_{-3}K_{\text{BH}}}{([\text{H}^+] + K_{\text{BH}})} \left( \frac{k_{-1}a_{\text{H}} + k_{-2}}{k_3 + k_{-2} + k_{-1}a_{\text{H}}} \right) \quad (3)
 \end{aligned}$$

These are related by the equilibrium constant  $K_{\text{obsd}} = k_{\text{hydro}}/k_{\text{form}}$ , and either formation or hydrolysis data may be used to give equivalent information. We have used both approaches as experimentally convenient. Steady-state data were analyzed according to these rate expressions using nonlinear least-squares regression procedures to give  $k_1$ ,  $k_2$ , and  $k_{-1}/k_3$ . Detailed balance allows subsequent calculation of  $k_{-3}$  and  $k_{-2}/k_3$ .

$k_3$  is obtained from analysis of the biphasic absorbance kinetics observed in stopped-flow experiments for reactions of this type.<sup>5,6</sup>

$$A(t) = A_0 + A_1 \exp(-r_1t) + A_2 \exp(-r_2t) \quad (4)$$

where  $r_1$  and  $r_2$  are cumbersome functions of the individual rate constants. It is straightforward, though algebraically tedious, to show that, for the hydrolysis direction in this case:

$$r_1r_2 = k_3(k_1a_{\text{H}} + k_2K_{\text{w}})/(a_{\text{H}} + K_{\text{SH}})$$

and, with  $k_1$  and  $k_2$  from steady-state data,  $k_3$  is determined.

**Resonance Raman.** Concentrated stock solutions of *N*-retinylidene-*n*-butylamine were made fresh daily by dissolution of retinal in ethanol containing 10 mM *n*-butylamine. Aliquots of this were subsequently diluted in aqueous 2% (by volume) Ammonyx, also containing 10 mM butylamine, to provide the unprotonated Schiff base sample (~0.3 mM) for Raman spectroscopy. Other components for the pH-jump experiments consisted again of 2% Ammonyx containing either 0.2 M HCl or 0.2 M sodium acetate buffer, pH 4–5. Final pH's in the reaction mixtures were measured after each experiment.

Polarized Raman spectra were obtained using an Applied Photophysics Model 36 multichannel instrument incorporating a Tracor Northern TN-1223-I cooled, intensified diode array detector with a TN-1710 mainframe and optical spectrometer module for data display and manipulation. Sample excitation was with the 457.9-nm line of a Spectra-Physics Model 171 argon ion laser with intensity, measured at the sample, of 100 mW or less, and a beam diameter approximately 0.2 mm (488- or 514-nm irradiation gave identical results, but with a higher fluorescent background). Experiments were carried out at room temperature (20 ± 1 °C). Continuous flow spectra were obtained in a 1-cm path-length quartz cell attached to a simple two-channel T-mixing device constructed of 1-mm bore Teflon tubing, with a dead-time under these conditions of about 10 s. Sample and pH-jump buffer solutions were pumped continuously at a combined flow rate of about 10 mL/min using separate

(4) (a) Provencher, S. W. *Biophys. J.* **1976**, *16*, 27. (b) Provencher, S. W.; Vogel, R. H. *Math. Biosci.* **1980**, *50*, 251.

(5) Espenson, J. H. *Chemical Kinetics and Reaction Mechanisms*; McGraw-Hill: New York, 1981.

(6) Fersht, A. R.; Jencks, W. P. *J. Am. Chem. Soc.* **1970**, *92*, 5432.

peristaltic pumps (LKB), giving a sample residence time in the laser beam of less than about 0.15 s. There was no evidence of photoisomerization of samples under these conditions. Trial experiments using the same configuration in a UV-visible spectrophotometer confirmed adequate mixing in this device. Raman spectra of the appropriate solvent mixtures were obtained using the identical flow system and subsequently subtracted from the sample spectra. All spectra consisted of 400 accumulations, with a 0.2-s acquisition time, at an instrumental bandwidth of 7  $\text{cm}^{-1}$  or less. Quoted wavenumbers are accurate to about 2  $\text{cm}^{-1}$  (indene calibration).

**Isotopic Labeling.** Bovine rod outer segment membranes (ROS) were isolated from the retinas of dark-adapted cattle eyes, obtained fresh locally, by standard techniques<sup>7</sup> and were stored frozen ( $-70^\circ\text{C}$ ) in the dark until use. Oxygen-18 enriched water (20 or 70% enrichment) was from Amersham International and *all-trans*-retinal from Fluka; all other reagents were of standard analytical grade. *N*-Retinylidene-*n*-butylamine was prepared as described above.

Retinal was isolated from freeze-dried ROS membranes (equivalent to 5–10 mg of rhodopsin) by repeated extraction with 5–10-mL aliquots of dry methylene chloride (dichloromethane).<sup>8</sup> Thorough mixing at each stage was obtained by passage through a glass syringe, and the supernatant was collected after centrifugation in a bench-top centrifuge (glass tubes); two to three extractions were found to be sufficient. Pooled extracts were concentrated in a stream of dry argon gas and purified by elution on preparative silica TLC plates with cyclohexane-ethyl acetate (3:1 by volume). The distinct yellow retinal band was redissolved in methylene chloride, concentrated under argon gas, and analyzed immediately by low resolution mass spectrometry (VG MS-12 linked to a PDP-8 computer, electron ionization 70 eV,  $10^{-7}$  torr). Instrumental controls included commercial *all-trans*-retinal and  $^{18}\text{O}$ -labeled retinal obtained by hydrolysis of synthetic *N*-retinylidene-*n*-butylamine in the presence of 20% enriched  $\text{H}_2^{18}\text{O}$ .

A typical experimental protocol was as follows: washed, unbleached bovine ROS membranes, containing 5–10 mg of rhodopsin, were freeze-dried (liquid nitrogen trap) and then bleached by exposure to 500-nm irradiation (100-W Xe/Hg lamp with interference filter), giving a color change from pink to deep orange, indicative of metarhodopsin I formation. Ice-cold  $\text{H}_2^{18}\text{O}$  (0.5 mL), buffered to pH 5.5 with sodium phosphate, was added (immediate color change from orange to pale yellow) and the sample maintained in the dark at  $0^\circ\text{C}$  for various periods between 30 s and 15 min prior to flash-freezing and freeze-drying. Retinal was then extracted and analyzed as described above. Control experiments following the same protocol included addition of  $\text{H}_2^{18}\text{O}$  buffered to pH 8 to the freeze-dried Meta I-ROS, and the brief bleaching of previously unbleached ROS incubated in  $\text{H}_2^{18}\text{O}$ , at pH 8,  $0^\circ\text{C}$ .

Infrared spectra (Perkin-Elmer 983) of the carbonyl stretch region were obtained by taking up the extracted retinals in carbon tetrachloride. Solvent backgrounds were subtracted separately.

## Results

**Model Studies: Equilibrium and Kinetics.** The absorbance spectrum of *all-trans*-retinal ( $\lambda_{\text{max}}$  380 nm) changes upon Schiff base formation to about 360 nm for the unprotonated imine and to 430–445 nm, depending on detergent, in the acidic form. This provides a convenient spectral probe for kinetic and equilibrium studies in the optically clear aqueous micelle mixtures. Equilibration of retinal with increasing concentrations of *n*-butylamine produces a progressive spectral shift with a single isosbestic point characteristic of simple stoichiometric reaction, and with no indication of thermal isomerization of the retinal. The absorbance changes, in most cases, give good linear Benesi-Hildebrand plots and a pH dependence of the apparent dissociation constant ( $K_{\text{obsd}}$ ) consistent with eq 2 (Figure 1). These data are consistent with previous estimates in neutral detergent<sup>9</sup> and show that the pH dependence of  $K_{\text{obsd}}$  is dominated by protonation of the amine. Essentially identical behavior is observed for neutral and cationic detergents, with only small differences in  $K_0$ , and the same value for  $\text{p}K_{\text{BH}} = 10.75$ , in agreement with literature values for *n*-butylamine in dilute aqueous solution<sup>10</sup> and with trial potentiometric titrations in the presence of the detergents (data not shown). A

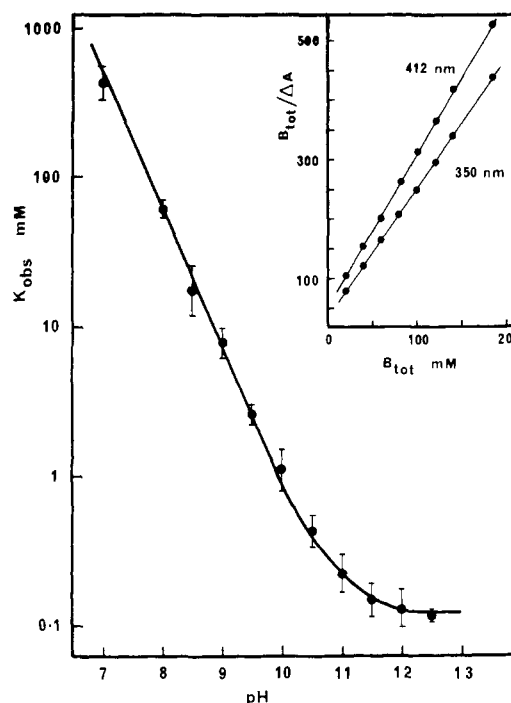


**Figure 1.** Observed dissociation constant ( $K_{\text{obsd}}$ ) as a function of pH for *N*-retinylidene-*n*-butylamine in 2% aqueous Emulphogene, determined from equilibrium absorbance changes ( $\Delta A$ ) over a range of butylamine concentrations ( $B_{\text{tot}}$ ). Inset: Example of the Benesi-Hildebrand plot of data at two different wavelengths for this system at pH 8.5.

**Table I.** Kinetic and Equilibrium Parameters for the Retinal/*n*-Butylamine Reaction in Detergent Micelles<sup>a</sup>

	Ammonyx	Emulphogene	DTAB	SDS
$\text{p}K_{\text{BH}}$	10.75	10.75	10.75	~11
$\text{pH}_{\text{mid}}$	4.85	6.1	5.84	9.54
$n$	0.77	1	0.77	1.1
$\text{p}\phi$	-2.37	0	-1.6	4.4
$K_0$ (mM)	0.22	0.13	0.25	~0.25
$k_1$ ( $\text{s}^{-1}$ )	0.31	$6.1 \times 10^{-4}$	$7.9 \times 10^{-3}$	~0.01
$k_2$ ( $\text{M}^{-1} \text{s}^{-1}$ )	$1.2 \times 10^4$	$2.0 \times 10^4$	$2.6 \times 10^4$	$\sim 3 \times 10^5$
$k_3$ ( $\text{s}^{-1}$ )	0.028	0.026	0.025	~0.05
$k_{-1}$ ( $\text{M}^{-1} \text{s}^{-1}$ )	$4.0 \times 10^5$	420	6500	$\sim 2 \times 10^5$
$k_{-2}$ ( $\text{s}^{-1}$ )	$1.1 \times 10^{-4}$	$9.4 \times 10^{-5}$	$1.5 \times 10^{-4}$	~0.05
$k_{-3}$ ( $\text{M}^{-1} \text{s}^{-1}$ )	124	371	153	~10
$k_1/k_{-1}$	$7.8 \times 10^{-7}$	$1.5 \times 10^{-6}$	$1.2 \times 10^{-6}$	$\sim 5 \times 10^{-8}$
$k_2/k_{-2}$	$1.1 \times 10^8$	$2.2 \times 10^8$	$1.7 \times 10^8$	$\sim 6 \times 10^6$
$k_3/k_{-3}$	$2.3 \times 10^{-4}$	$7.0 \times 10^{-5}$	$1.6 \times 10^{-4}$	$\sim 5 \times 10^{-3}$

<sup>a</sup> Except as indicated for SDS, where only order-of-magnitude estimates are available, typical maximum estimated error limits are as follows:  $\text{p}K_{\text{BH}}$ ,  $\text{pH}_{\text{mid}}$ ,  $n$ ,  $\text{p}\phi$  ( $\pm 0.05$ );  $K_0$  ( $\pm 10\%$ ); rate constants ( $\pm 20\%$ ).

major exception occurs in the case of the strongly anionic SDS where the Benesi-Hildebrand plots are distinctly nonlinear and poorly reproducible, indicating a more complex equilibrium process. pH titration of butylamine in the presence of SDS gives anomalous  $\text{p}K$ 's in excess of 11, suggestive of some specific SDS-butylamine interaction or of partitioning of the amine into the SDS micelles. This concentration-dependent effect will clearly affect the apparent equilibrium of the retinal Schiff base reaction, but we have not so far investigated the phenomenon any further. An estimate of  $K_0$  in this case was obtained from comparison of formation and hydrolysis rates at high pH and does not differ significantly from the other detergents (Table I).

Spectral acid-base titrations of the retinyl Schiff base in different detergents are illustrated in Figure 2, plotted using the procedure described in the Experimental Section. There are significant differences in apparent  $\text{p}K$  of the retinyl Schiff base in different micelles, correlating qualitatively with the ionic state of the detergent. The apparent  $\text{p}K$  in Emulphogene,  $\text{pH}_{\text{mid}}$  6.1, is in good agreement with previous estimates under similar conditions in other neutral detergents,<sup>11,12</sup> but somewhat lower values

(7) Papermaster, D. S.; Dreyer, W. J. *Biochemistry* **1974**, *13*, 2438.

(8) Seltzer, S.; Lin, M. *Methods Enzymol.* **1982**, *88*, 542.

(9) De Pont, J. J. H. M.; Daemen, F. J. M.; Bonting, S. L. *Arch. Biochem. Biophys.* **1970**, *140*, 267.

(10) (a) Christensen, J. J.; Izatt, R. M.; Wrathall, D. P.; Hansen, L. D. *J. Chem. Soc. A* **1969**, 1212 (adjusted to  $20^\circ\text{C}$ ). (b) Perrin, D. D.; Dempsey, B.; Serjeant, E. P. *pK Prediction for Organic Acids and Bases*; Chapman & Hall: London, 1981.

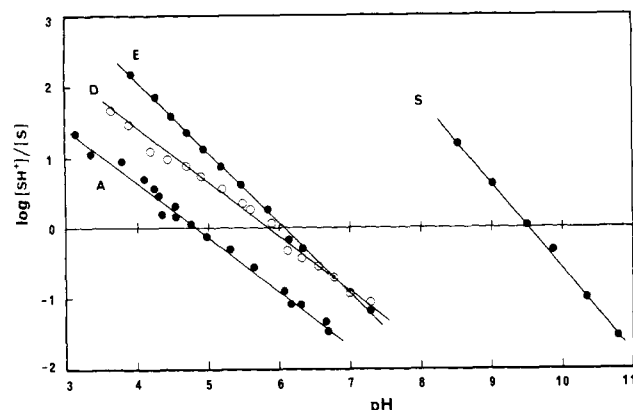


**Figure 2.** pH titrations of *N*-retinylidene-*n*-butylamine in Ammonyx (A), Emulphogene (E), DTAB (D), and SDS (S): determined from the initial absorbances during pH-jump stopped-flow experiments and plotted according to eq 1.

(4.85 and 5.84, respectively) are found for Ammonyx and DTAB; a dramatically higher value is found (9.54) in SDS. Similar alterations in apparent  $pK_a$ 's in the presence of charged micelles have been reported elsewhere<sup>12</sup> and, bearing in mind that the weakly basic amine oxide detergent, Ammonyx, will itself become protonated below neutral pH, these observations are consistent with simple electrostatic effects on Schiff base protonation and/or hydrogen ion activity in the micellar environment.<sup>12a,d</sup> The magnitude of the  $pK$  shift in SDS suggests the possibility of specific ionic interaction between the polar sulfonic acid head group and the imine nitrogen, in this case, rather than a delocalized non-specific effect of micellar surface potential. This is reminiscent of the SDS-butylamine interaction postulated above.

Although the titration plots of Figure 2 are all reasonably linear, only in the case of Emulphogene does the slope ( $n$ ) equal unity. Shallower titrations ( $n = 0.77$ ) are seen for the Schiff base in Ammonyx or DTAB, and sharper ones ( $n = 1.1$ ) in SDS. We have no general explanation for this phenomenon, though it is consistently observed using various buffers and absorbance wavelengths. In the case of Ammonyx, protonation in a similar pH region and the associated changes in micelle surface potential would attenuate the Schiff base titration, but this would not apply with SDS or DTAB. This nonideality may possibly reflect changes in micelle potential due to ionic strength changes in the buffer counterions during titration. Unfortunately, because of the poor solubility of the detergents at high ionic strengths, we were unable to test this possibility. However, in some experiments in SDS, in which the buffer also contained 10 mM butylamine (in an attempt to suppress hydrolysis, data not shown), the apparent  $pK$  was reduced slightly to about 9.3 (compared to 9.54) and the slope closer to 1. Other experiments, mentioned above, on the acid-base titration of butylamine itself in the presence of SDS have shown anomalies suggesting some specific interaction between SDS and the protonated butylamine. This indicates that the anomalous titration behavior that we have observed is associated with the charge density at the micelle surface and probably involves counterion effects.

The pH dependence of the state of ionization of the retinyl imine is required for quantitative analysis of the reaction kinetics in terms of the carbinolamine intermediate mechanism. In the absence of any appropriate theoretical expression, the data of Figure 2 suggest an empirical equation (eq 1, Experimental Section) which adequately expresses the apparent micellar hydrogen ion activity as a function of measured pH. This, together with experimental parameters given in Table I, is used in the steady-state rate expressions to describe the Schiff base protonation in different

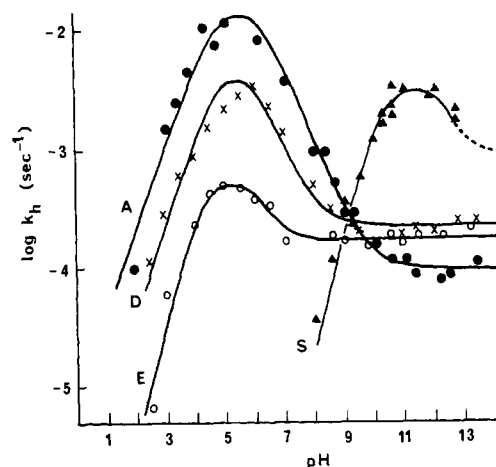


**Figure 3.** Steady-state pH-rate profiles for hydrolysis of *N*-retinylidene-*n*-butylamine in aqueous detergent mixtures at 20 °C: (A) Ammonyx, (E) Emulphogene, (D) DTAB, (S) SDS. The solid lines are theoretical profiles plotted according to the carbinolamine mechanism using the parameters listed in Table I. Except for SDS, points above pH 8 are obtained from formation rate data.

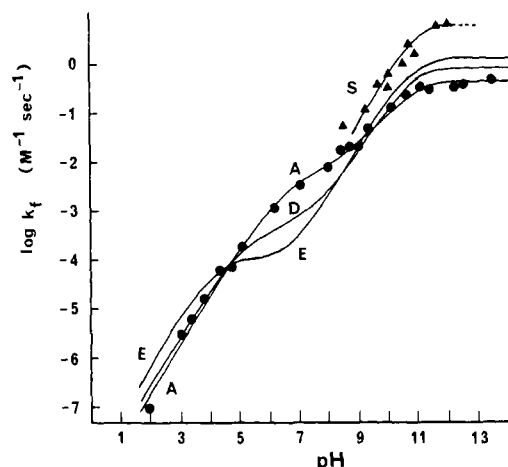
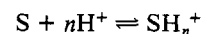


**Figure 4.** Steady-state pH-rate profiles for formation of *N*-retinylidene-*n*-butylamine in aqueous detergent mixtures at 20 °C: (A) Ammonyx, (E) Emulphogene, (D) DTAB, (S) SDS. The solid lines are theoretical profiles for second-order formation rates according to the carbinolamine mechanism using the parameters from Table I. Data below pH 8 are calculated from hydrolysis rates under these conditions. Data points for DTAB and Emulphogene give equally good fits to the theoretical curves, but have been omitted for clarity.

detergents. It is worth noting here that this empirical relation is formally equivalent to a nonstoichiometric, or fractional protonation scheme:



with a dissociation constant,  $K = [S][H^+]^n/[SH_n^+]$ . Interestingly, such apparent "fractional protonation" behavior has been observed on many occasions as a feature of the acid-base equilibrium of the metarhodopsin intermediates of visual pigment photolysis,<sup>13</sup> where it presumably reflects a similar nonideality in titration behavior of groups within the protein environment.

Steady-state rate constants for hydrolysis and formation of the model Schiff base as a function of pH in the different detergents, shown in Figures 3 and 4, display all the general features expected of the carbinolamine intermediate mechanism, although there are significant quantitative variations induced by the different micelle

(11) Blatz, P. E.; Johnson, R. H.; Mohler, J. H.; Al-Dilaimi, S. K.; De-whurst, S.; Erickson, J. O. *Photochem. Photobiol.* **1971**, *13*, 237.

(12) (a) Hartley, G. S.; Roe, J. W. *Trans. Faraday Soc.* **1949**, *36*, 101. (b) Behme, M. T. A.; Cordes, E. H. *J. Am. Chem. Soc.* **1965**, *87*, 260. (c) Kito, Y.; Nashima, K. *Photochem. Photobiol.* **1980**, *32*, 443. (d) Romsted, L. S. *J. Phys. Chem.* **1985**, *89*, 5107.

(13) (a) Parkes, J. H.; Liebman, P. A. *Biochemistry* **1984**, *23*, 5054. (b) Matthews, R. G.; Hubbard, R.; Brown, P. K.; Wald, G. *J. Gen. Physiol.* **1963**, *47*, 215. (c) Abrahamson, E. W.; Wiesenfeld, J. R. In *Handbook of Sensory Physiology*; Dartnall, H. J. A., Ed.; Springer-Verlag: West Berlin, 1972; Vol. VII, Part 1, p 69. (d) Abrahamson, E. W.; Fager, R. S. *Curr. Top. Bioenerg.* **1973**, *5*, 125.

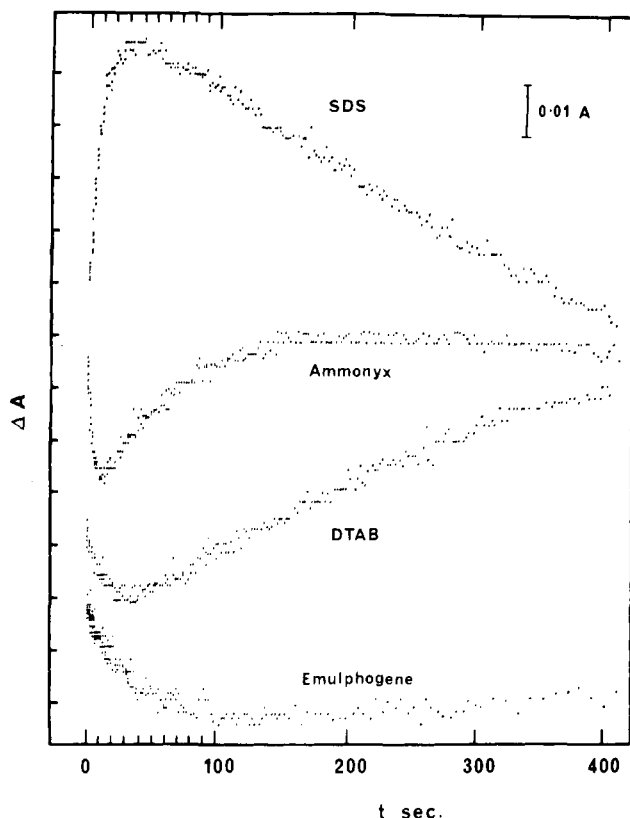


**Figure 5.** Examples of stopped-flow data showing transient absorbance changes during the initial stages of hydrolysis of *N*-retinylidene-*n*-butylamine in SDS (360 nm, pH 11), Ammonyx (370 nm, pH 5), DTAB (370 nm, pH 5.5), and Emulphogene (370 nm, pH 6).

environments. Despite these differences, provided due account is taken of the abnormal Schiff base protonation behavior, steady-state pH-rate profiles are adequately described by the appropriate rate expressions (eq 3) and, in most cases, yield the unambiguous sets of rate parameters listed in Table I. Again, however, SDS is an exception where because of the limited pH range over which rate data were accessible, and also possibly because of interference from specific interactions, no stable set of parameters emerged from the least-squares fitting procedures and only rough orders of magnitude estimates are given. Nevertheless, the overall shape of the SDS rate profiles are clearly in line with the general mechanism, though dominated by the large pK shift of the imine in this environment.

Direct evidence for the tetrahedral intermediate comes from rapid-mixing hydrolysis experiments. Transient accumulation of the carbinolamine intermediate during hydrolysis is optimal near the peak of the pH profile. Stopped-flow experiments over a wide range of wavelengths in this pH region, examples of which are given in Figure 5, in all cases showed the biphasic behavior characteristic of the buildup and decay of the intermediate species, and the kinetic data are well described by the anticipated double-exponential expression (eq 4). Rate constants for the fast phase ( $r_1$ ) ranged from about 0.02 to 0.3 s<sup>-1</sup>, depending on pH and detergent, while the slower phases ( $r_2$ ) were identical with steady-state rates under the same conditions. Analysis of  $r_1$  values in conjunction with the steady-state results gave the additional information required for complete determination of the mechanistic rate constants (Table I). The absorbance spectrum of the intermediate, estimated from the amplitudes of the different kinetic phases in these experiments (not shown), depends on pH and is very similar in form to the parent Schiff base, indicating only changes in extent of protonation, or small variations in extinction coefficient, rather than gross changes in absorbance maxima. Assuming that a red shift is indicative of protonation of the carbinolamine, as it is with the Schiff base, then the transient spectral changes are consistent with an increase in protonation at low pH and a decrease at higher pH (in SDS), placing the

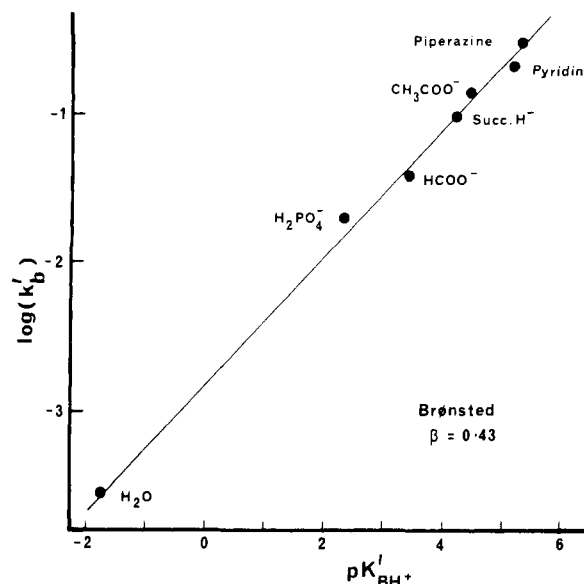


**Figure 6.** Statistically corrected Brønsted plot of general base catalysis constants ( $k'_b$ ) as a function of conjugate acid dissociation constants ( $K'_{BH}$ ) for hydrolysis in Emulphogene. General bases used included formate, acetate, succinate, phosphate, pyridine, and piperazine, as indicated.

carbinolamine pK<sub>a</sub> somewhere in the region 7–9, as might be expected.<sup>10b</sup> Estimation of the steady-state accumulation of the intermediate shows that, in most cases, the buildup is no greater than about 5% of the total Schiff base concentration, and usually very much less. In Ammonyx, however, the relatively high value of  $k_1$  (discussed below) favors kinetic accumulation of the intermediate under suitable pH conditions, such that an estimated 50% of the Schiff base may be present as the carbinolamine during the early stages of hydrolysis at pH 4–5. No rapid transients are observable during hydrolysis away from the pH maxima, nor under any accessible conditions during the formation reaction. The latter observation is consistent with the mechanism in which nucleophilic attack by the amine on the aldehyde is rate-limiting in the observable pH range.

Steady-state hydrolysis rates in Emulphogene over the pH range 4–6, where attack of water on the protonated Schiff base is rate limiting, showed variations with buffer type and concentration typical of general base catalysis with a Brønsted coefficient  $\beta$  of about 0.43 (Figure 6), which is reasonable for reactions of this type.<sup>14</sup> However, no such effect was seen in Ammonyx. On examination of the rate parameters of Table I, we note that  $k_1$ , the rate constant for the base-catalyzed step, is significantly higher for Ammonyx than for the other detergents, suggesting that in these micelles the hydrolysis reaction is already experiencing significant base catalysis from the amine oxide head groups of the detergent and that this is sufficient to mask any possible further catalysis from general bases in solution. Support for this comes from the observation that, discounting SDS which seems to be a special case throughout, the ratio  $k_1/k_{-1}$  is reasonably constant over the range of detergents, despite wide variations in the absolute values of the individual rate constants. Thus, any specific micelle interactions seem to have an equal effect on the magnitudes of both the forward and reverse rate constants of this step, in a manner characteristic of a catalytic process rather than a change in thermodynamic equilibrium stability of any of the reactant species. Similar conclusions may be drawn about the other steps of the mechanism where  $k_2/k_{-2}$  and  $k_3/k_{-3}$  also show little variation, though here the rate constants themselves vary only marginally with detergent.

Hydrolysis in Ammonyx micelles using D<sub>2</sub>O, pD 4.0, as solvent was significantly slower than under identical conditions in H<sub>2</sub>O, giving a solvent isotope effect,  $k^H/k^D$ , of about 2.3. This is close

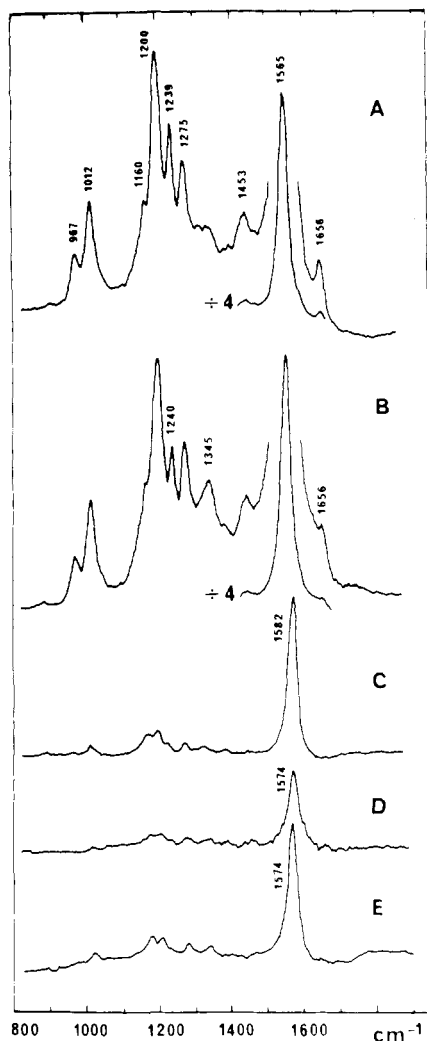


**Figure 7.** Continuous-flow, pH-jump resonance Raman spectra (100 mW, 457.9 nm excitation, solvent background subtracted) of *N*-retinylidene-*n*-butylamine and its hydrolysis products in 2% aqueous Ammonyx mixtures: (A) protonated Schiff base in 0.1 M HCl; (B) Schiff base approximately 10 s after pH jump to pH 4.2; (C) unprotonated Schiff base in 10 mM butylamine; (D) Schiff base total hydrolysis products, approximately 20 min after pH jump to pH 4.2; (E) *all-trans*-retinal in pH 4 buffer. All spectra were run consecutively under identical instrumental conditions with the same total retinal concentration, and are shown to scale (except where indicated) in order to illustrate the different extents of resonance enhancement.

to the value observed in other studies of Schiff base hydrolysis<sup>14</sup> where it has been interpreted mechanistically in terms of a close resemblance of the transition state to the protonated carbinolamine.<sup>14,15</sup>

**Resonance Raman Spectroscopy.** Continuous-flow Raman data on *N*-retinylidene-*n*-butylamine and its hydrolysis products, under various conditions in aqueous Ammonyx dispersions, are summarized in Figure 7. Spectra in 0.1 M HCl show intense resonance enhancement, with a strong retinal C=C stretch band at 1565 cm<sup>-1</sup>, a protonated imine C=N stretch at 1656 cm<sup>-1</sup>, and major fingerprint vibrations in the 1100–1400-cm<sup>-1</sup> region characteristic of the protonated *all-trans*-retinal Schiff base<sup>16</sup> (Figure 7A). Hydrolysis is essentially nonexistent under these conditions and most of the assigned bands in the high-resolution spectra of the crystalline protonated *n*-butylamine Schiff base<sup>16</sup> can be identified, albeit at lower resolution. Significant changes in this spectrum occur, however, during the early stages of hy-

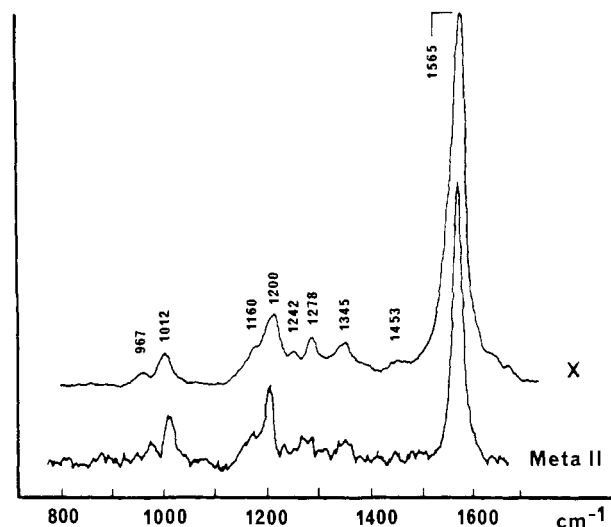


**Figure 8.** Resonance Raman spectrum of the tetrahedral carbinolamine intermediate (X) of hydrolysis of *N*-retinylidene-*n*-butylamine in aqueous Ammonyx micelles, pH 4–5, derived by subtraction of the protonated Schiff base component from continuous-flow spectra during the early stages of hydrolysis. The metarhodopsin II spectrum, for comparison, is redrawn on the same wavenumber scale from ref 17a. The major peak positions in these spectra are identical within instrumental resolution.

drolysis (Figure 7B), approximately 10 s after pH jump of the unprotonated imine to the pH 4–5 region (0.1 M acetate buffer, final concentration). In particular, there is a marked decrease in intensity of the 1240- and 1656-cm<sup>-1</sup> bands, compared to the protonated Schiff base, together with the appearance of a prominent band at about 1345 cm<sup>-1</sup>. We ascribe these changes to the buildup of the tetrahedral carbinolamine intermediate of imine hydrolysis, which the kinetic studies have shown to be optimal under these conditions. Similar effects are seen using various laser excitation lines and, to a lesser extent, using the detergent Emulphogene instead of Ammonyx. None of these features, especially the 1345-cm<sup>-1</sup> peak, appear in Raman spectra of the unprotonated Schiff base or retinal hydrolysis products run under identical conditions (Figure 7C–E). Such spectra, furthermore, show considerably less resonance enhancement because of the hypsochromic shift of these pigments relative to the exciting line (absorbance maxima: 380 and 360 nm approximately for retinal and the unprotonated Schiff base, respectively, compared to about 440 nm for the protonated imine). Moreover, any significant contamination from such sources during the early stages of hydrolysis would give rise to a shift in the 1565-cm<sup>-1</sup> C=C band. No such shift is observed. In any case, the kinetic studies indicate that the Schiff base is predominantly protonated at pH 4 to 5 and that less than 10% complete hydrolysis occurs within 10 s under these conditions.

The Raman spectrum Figure 7B consists, therefore, of a mixture of the tetrahedral carbinolamine intermediate of the imine hydrolysis reaction together with unreacted protonated Schiff base, in roughly equal proportions as judged from the appropriate rate expressions under these conditions. Subtraction of 50% of the protonated imine spectrum (Figure 7A) yields an estimate of the Raman spectrum of the pure intermediate (Figure 8), and this, to our knowledge, represents the first such spectrum reported for any transient carbinolamine. The spectrum retains many of the major features of the protonated Schiff base, but with the significant loss of the 1240- and 1656-cm<sup>-1</sup> bands and the presence, already noted, of the new band at 1345 cm<sup>-1</sup>. In the absence of any small-molecule carbinolamine spectra for comparison, we can make no firm assignment for this vibration, apart from noting that its frequency is consistent with the alcoholic O–H in-plane deformation that might be expected in the carbinolamine, though, by analogy with the complex vibrational behavior of amide groups, we should not necessarily expect the spectrum of this linkage to be simply a superposition of amine and alcoholic characteristic group frequencies because of potential coupling between the modes.

(15) Archila, J.; Bull, H.; Langenaur, C.; Cordes, E. H. *J. Org. Chem.* **1971**, *36*, 1345.

(16) Smith, S. O.; Myers, A. B.; Mathies, R. A.; Pardo, J. A.; Winkel, C.; Van den Berg, E. M. M.; Lugtenburg, J. *Biophys. J.* **1985**, *47*, 653.

**Table II.** Low-Resolution Mass Spectra of Retinals. Relative Abundances in the Molecular Ion Region, Normalized to the  $m/z$  284 Peak

retinal sample <sup>a</sup>	284	$m/z$ 285	286
A	1	0.24	0
B	1	0.23	0.14
C	1	0.23	0
D	1	0.25	0
E	1	0.24	0.69
F	1	0.28	0.42

<sup>a</sup> (A) Commercial, natural abundance *all-trans*-retinal. (B) Retinal after hydrolysis from *N*-retinylidene-*n*-butylamine in 20% enriched  $H_2^{18}O$ . (C) Extracted from Meta I-ROS incubated for 10–15 min in 70% enriched  $H_2^{18}O$  at pH 8, 0 °C. (D) Extracted from ROS membranes, preequilibrated in 70%  $H_2^{18}O$  and bleached to the Meta I stage at pH 8, 0 °C. (E) Extracted from ROS membranes after a 30-s exposure to 70%  $H_2^{18}O$  during the Meta I  $\rightarrow$  II transition, pH 5.5, 0 °C. (F) As in E, but with a 10-min exposure to labeled water.

(Deuterium-labeling experiments, though attempted, were not helpful here because the kinetic isotope effect in  $D_2O$  diminishes the transient levels of the carbinolamine to below detectable limits in these spectra.) The  $1656\text{-cm}^{-1}$  band is predominantly due to modes associated with the protonated  $C=N$  bond of the imine,<sup>16</sup> and its disappearance is entirely consistent with conversion of this group to a carbinolamine linkage. Assignment of the band at about  $1240\text{-cm}^{-1}$  in the protonated Schiff base is not entirely certain, though it seems to be a highly mixed combination of  $C-C$ ,  $C=C$ ,  $C-CH_3$  stretch vibrations and CCH in-plane rocks involving several carbons, including C-15.<sup>16</sup> It is not unreasonable, therefore, that alcoholic substitution on C-15 might significantly affect this mode. We note, however, that the intensity of this band appears somewhat greater in our detergent-solubilized spectra than in the solid state,<sup>16</sup> and this might reflect possible conformational differences between the protonated Schiff base in the micelle and the crystal which could affect mode assignment.

But, regardless of the precise mode assignments, the most surprising feature of the carbinolamine spectrum is its remarkable similarity to the published spectrum of the metarhodopsin II photoproduct of bovine rhodopsin,<sup>17</sup> most notably in the presence of the hitherto unexplained  $1345\text{-cm}^{-1}$  peak (Figure 8). The ramifications of this observation in relation to the hydrolysis step of rhodopsin photolysis are considered below.

**$^{18}O$  Labeling Studies.** The starting point for these experiments was the early observation that, in the absence of water, bleaching of rhodopsin does not proceed further than the metarhodopsin I intermediate.<sup>18</sup> In our hands, freeze-dried bovine rod outer segments are pale pink, changing to a stable orange color (Meta I) on exposure to light. This color persists on addition of ice-cold pH 8 buffer, whereas pH 5.5 buffer gives an immediate change to pale yellow (Meta II). Both these intermediates are stable for many minutes at 0 °C in water,<sup>13b,19</sup> and for much longer if immediately freeze-dried.

Low-resolution mass spectra of unlabeled retinals, either commercial material or that extracted from fully bleached freeze-dried ROS, show typical fragmentation patterns with a major parent ion peak at  $m/z$  284, and a minor peak at 285 arising mainly from natural abundance carbon-13 (Table II; samples A, C, and D).<sup>8</sup> The absence of any higher mass ions, together with a constant 285/284 ratio of  $0.24 \pm 0.02$ , confirms the lack of potential interference from retinol or retinoic acid in these preparations. By contrast, in preliminary trials using retinal extracted from ROS fully bleached in aqueous buffers slightly enriched in  $^{18}O$ , or from hydrolyzed synthetic retinal Schiff base in the same medium (Table II; sample B), an additional peak at 286 was observed, consistent with the anticipated hydrolytic incorporation of  $^{18}O$  in the aldehydic  $C=O$  group. This confirmed the feasibility of

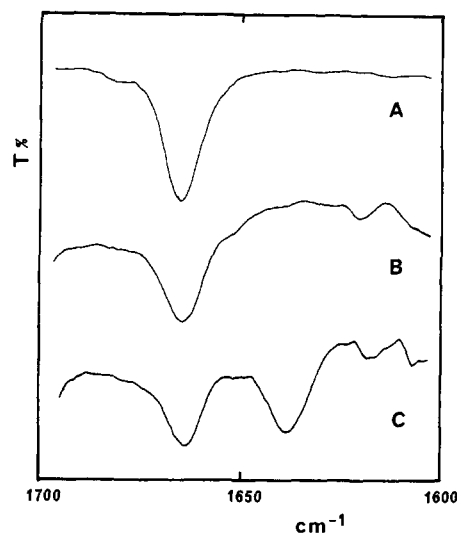


**Figure 9.** Superimposed tracings of infrared spectra in the carbonyl-stretch region, solvent background ( $CCl_4$ ) subtracted, arbitrary % transmission scale: (A) commercial *all-trans*-retinal; (B) retinal extracted from bleached ROS membranes; (C) retinal extracted from ROS membranes exposed to 70% enriched  $H_2^{18}O$  at the Meta I  $\rightarrow$  Meta II stage.

a more detailed study of the effect of  $H_2^{18}O$  specifically at the metarhodopsin stage of bleaching. Data obtained using more highly enriched  $H_2^{18}O$  are also shown in Table II.

Bleaching of ROS in isotopically enriched water under conditions favoring Meta I formation (pH 8, 0 °C), or addition of  $H_2^{18}O$  to dried Meta I containing ROS under the same conditions, gives molecular ion ratios of the extracted retinals identical with natural abundance spectra (Table II; samples C and D). However, addition of  $H_2^{18}O$  to dried Meta I-ROS under conditions favoring transition to Meta II gives rise to a large additional peak at  $m/z$  286 (samples E and F). Previous studies<sup>13b,19</sup> have shown that in ROS membranes at 0 °C the metarhodopsin photoproducts are relatively stable under appropriate pH conditions (pH 8 for Meta I, pH 5.5 for Meta II). Transformation of Meta II to subsequent intermediates is very slow (minutes–hours) under these conditions, and  $^{18}O$  incorporation varied little with  $H_2^{18}O$  incubation time in our experiments. In fact, yields of the 286 parent ion were somewhat lower for the longer incubation times, possibly due to exchange with atmospheric moisture or because subsequent intermediate stages (Meta III, indicator yellow) involve re-formation of retinal–imine linkages. The 285/284 ratios remained constant in all these experiments, ruling out the possibility of artifacts due to retinal oxidation products. Relative yields of  $m/z$  286 ions were always less than expected from the (nominal) 70% enrichment of the labeled water. It is not clear whether this is due to extraneous retinal from partial bleaching of the starting material, incomplete initial photoreaction of the rhodopsin, differences in the fragmentation ratios of labeled and unlabeled retinals, or isotopic dilution from residual water in the freeze-dried samples. Nevertheless, these experiments clearly demonstrate significant  $^{18}O$  uptake from  $H_2^{18}O$  during the Meta I  $\rightarrow$  Meta II transition, but not earlier.

If  $^{18}O$  incorporation is indeed due to hydrolysis, then, clearly, the expected site of incorporation must be the carbonyl oxygen of the aldehyde, and this is supported by IR spectra of extracted retinals in the carbonyl-stretch region (Figure 9). Unlabeled retinals show the usual strong  $C=O$  band at  $1664\text{-cm}^{-1}$ , whereas retinal extracted under  $^{18}O$ -labeling conditions gives an additional band at about  $1638\text{-cm}^{-1}$ . This shift is consistent with a simple isotope effect on the  $C=O$  stretch vibration due to an increased reduced mass of the  $C=O$  group, and agrees with published shifts in other  $^{18}O$ -labeled aldehydes.<sup>20</sup>

(17) (a) Doukas, A. G.; Aton, B.; Callender, R. H.; Ebrey, T. G. *Biochemistry* **1978**, *17*, 2430. (b) Pande, J.; Pande, A.; Callender, R. H. *Photochem. Photobiol.* **1982**, *36*, 107.

(18) (a) Wald, G.; Durrill, J.; St. George, R. C. C. *Science* **1950**, *111*, 179. (b) Rafferty, C. N.; Shichi, H. *Photochem. Photobiol.* **1981**, *33*, 229.

(19) Cooper, A.; Converse, C. A. *Biochemistry* **1976**, *15*, 2970.

(20) Pinchas, S.; Laulicht, I. *Infrared Spectra of Labelled Compounds*; Academic Press: London, 1971.



## Discussion

Three significant conclusions, bearing on the stability and photolysis of rhodopsins and related proteins, have been established by the experiments reported here. Firstly, although the precise behavior may be modulated by environmental effects, model retinal Schiff base formation and hydrolysis conforms in all respects to the conventional tetrahedral carbinolamine reaction mechanism so that we may, with some confidence, begin to interpret some of the apparently anomalous properties of the rhodopsin chromophore. Secondly, the resonance Raman spectrum of this transient carbinolamine intermediate is virtually identical with the spectrum of the metarhodopsin II intermediate encountered during bleaching of bovine rhodopsin. Finally, retinal extracted from bovine photoreceptor membranes after exposure to  $\text{H}_2^{18}\text{O}$  solely during the Meta I to Meta II transition shows isotope uptake at the carbonyl oxygen position. Taken together, these last two observations support the hitherto unconventional view<sup>19</sup> that the metarhodopsin transition marks the start of the chromophore hydrolysis step of visual pigment photolysis.

Prior to this work there was considerable circumstantial evidence that chromophore hydrolysis might be involved as early as the metarhodopsin stage. For example, (i) water is required for the photoreaction to proceed beyond Meta I;<sup>18</sup> (ii) metarhodopsin is the first stage at which the retinyl chromophore becomes accessible to water-soluble reagents such as hydroxylamine and sodium borohydride,<sup>21</sup> and it is not unreasonable to presume similar accessibility to water itself; (iii) the transition from Meta I to Meta II is the only spontaneous endothermic step of the bleaching sequence (+10 kcal/mol),<sup>19,22</sup> and the energetics are consistent with Schiff base hydrolysis enthalpies in model compounds (8–12 kcal/mol);<sup>19</sup> (iv) the kinetics and equilibrium of the Meta I  $\rightarrow$  Meta II transition are complex, involving asynchronous and anomalous protonation changes<sup>13,23</sup> and possible base catalysis<sup>13a</sup> that are reminiscent of the features observed here in the hydrolysis of model retinal Schiff bases; (v) the 380-nm absorbance maximum of Meta II is the same as free retinal. This was first noted in the original work on metarhodopsin tautomerism,<sup>13b</sup> though the authors ruled out hydrolysis at this stage mainly on the basis of rapid reversibility to Meta I and on the photoreversibility of Meta II to the parent rhodopsin. But this rests on the mistaken assumption that hydrolysis of the chromophore linkage is synonymous with release from the active site. If, as indicated by the present work, the hydrolyzed chromophore in Meta II still resides in the specific retinal binding site of opsin, then such considerations are no longer a problem.

Our experiments are not necessarily unambiguous. Although control experiments using the same protocol but without Meta II formation give no isotope labeling, it might be argued that the  $^{18}\text{O}$  incorporation results are an artifact of the extraction procedure rather than indicators of in situ attack by water. This seems unlikely in view of the resonance Raman data (Figure 8) showing remarkable similarity between the spectrum of the initial product of Schiff base hydrolysis and that of authentic metarhodopsin II. But even here some caution must be exercised since the Meta II Raman spectrum has itself been the subject of some controversy,<sup>17,24</sup> with Callender's group arguing strongly that it supports the conventional view of metarhodopsin II as the unprotonated retinal Schiff base<sup>17</sup> despite (a) the lack of any feature corresponding to the C=N stretch,<sup>24</sup> (b) the closer correspondence of the 1569-cm<sup>-1</sup> C=C stretch of Meta II with retinal (1574 cm<sup>-1</sup>) and, now, the carbinolamine (1564 cm<sup>-1</sup>) rather than the unprotonated imine (1582 cm<sup>-1</sup>); and (c) without any assignment for the 1345-cm<sup>-1</sup> band. There are also some experimental un-

certainities involved in correcting for residual Meta I in the sample,<sup>17</sup> and it is conceivable that this spectrum also contains preferentially enhanced features from other unidentified species isochromic with Meta I. Nevertheless, the weight of experimental evidence now indicates that hydrolysis of the retinal Schiff base linkage of rhodopsin starts at the metarhodopsin stage of bleaching, and that Meta II probably represents, at least in part, a stabilized form of the tetrahedral carbinolamine species in the retinal binding site.

If this is so, then it implies the existence of some unusual specific interactions in the retinal binding site of rhodopsin, some of which may be inferred from the properties of opsin and the unbleached pigment. The model studies have established that under normal circumstances a stable retinal Schiff base forms only with an unprotonated amine group, and the resultant imine bond becomes susceptible to hydrolysis upon protonation.<sup>25</sup> But visual pigment and related chromophores are stable over a wide pH range, and pigment regeneration by recombination of the appropriate retinal isomer with opsin<sup>26</sup> or bacteriorhodopsin<sup>27</sup> is rapid and spontaneous at physiological pH. We therefore infer that the active site lysine is unprotonated, or only partially protonated, at physiological pH, with an anomalously low  $pK_a$  that allows rapid and thermodynamically stable Schiff base formation. This is in agreement with studies on the energetics and protonation states of bovine rhodopsin,<sup>19</sup> and with the protonation changes during reconstitution of bacteriorhodopsin.<sup>28</sup> There are precedents in other proteins as well: in the Schiff base enzyme acetoacetate decarboxylase,<sup>29</sup> for instance, it has been established by chemical techniques that the active lysine has a similarly low  $pK_a$ . Among the various noncovalent interactions within the protein active site, only the Coulombic effects of close proximity with cationic groups (arginine or additional lysine residues, for example) can be reasonably responsible for such dramatic reductions in the  $pK_a$  of the active lysine.<sup>19,29</sup> (Interaction with a histidine residue seems less likely since imidazole is normally a much weaker base and probably would not dominate an electrostatic interaction with an adjacent primary amine.) This is not inconsistent with the possible disposition of several basic amino acid residues within the protein structure, as suggested from analysis of the primary sequence.<sup>1f</sup> Simple calculations,<sup>30</sup> together with experimental data on diamines,<sup>10</sup> indicate that a single positive charge within a few ångströms of an amino group is sufficient to reduce the  $pK$  by the required 3–4 units.

Barring any major conformational changes, the same active site contacts should persist in the presence of retinal and should similarly depress the  $pK$  of the chromophoric imine. Yet, according to most spectroscopic criteria, the Schiff bases of rhodopsins appear to be protonated,<sup>1</sup> and remain so in the unbleached pigment over a wide pH range. The imine  $pK_a$  in bacteriorhodopsin has been measured<sup>31</sup> at about 13.3 and, although not yet determined, is likely to be similarly high in the visual rhodopsins. This anomalously high  $pK$  is opposite to what should be expected from simple electrostatic effects of adjacent cationic groups. While it is tempting at this stage to suppose that there are indeed major conformational differences between opsin and rhodopsin which alter the disposition of charged groups in the

(25) As also shown by the pioneering work of the Liverpool group: (a) Morton, R. A.; Pitt, G. A. *J. Biochem. J.* **1955**, *59*, 128. (b) Pitt, G. A. J.; Collins, F. D.; Morton, R. A.; Stok, P. *Ibid.* **1955**, *59*, 122.

(26) Henselman, R. A.; Cusanovich, M. A. *Biochemistry* **1976**, *15*, 5321.

(27) Oesterhelt, D.; Schühmann, L. *FEBS Lett.* **1974**, *44*, 262.

(28) Fischer, U. C.; Oesterhelt, D. *Biophys. J.* **1980**, *31*, 139 (though these authors rejected the low- $pK_a$ -lysine hypothesis on the basis of the paradoxical consequences for Schiff base protonation).

(29) Kokesh, F. C.; Westheimer, F. H. *J. Am. Chem. Soc.* **1971**, *93*, 7270.

(30) Electrostatic repulsion between two single point charges, with separation  $R$  Å in a medium of dielectric constant  $D$ , gives  $\Delta pK = -240/DR$ , approximately. The value of  $D$  within the protein matrix has recently been estimated to be in the range 2.5 to 4 (Gilson, M. K.; Honig, B. H. *Biopolymers* **1986**, *25*, 2097). The potentially large  $pK$  shifts arising thus from a proximal positive charge will be partially offset by a possible nearby negative group, discussed later.

(31) (a) Druckmann, S.; Ottolenghi, M.; Pande, A.; Pande, J.; Callender, R. H. *Biochemistry* **1982**, *21*, 4953. (b) Sheves, M.; Albeck, A.; Friedmann, N.; Ottolenghi, M. *Proc. Natl. Acad. Sci. U.S.A.* **1986**, *83*, 3262.

(21) (a) Bownds, D.; Wald, G. *Nature (London)* **1965**, *205*, 254. (b) Akhtar, M.; Blasse, P. T.; Dewhurst, P. B. *Biochem. J.* **1968**, *110*, 693. (c) Ratner, V. L.; Bagirov, I. G.; Fesenko, E. E. *Vision Res.* **1981**, *21*, 251.

(22) (a) Cooper, A. *Nature (London)* **1979**, *282*, 531. (b) Cooper, A. *FEBS Lett.* **1981**, *123*, 324. (c) Cooper, A.; Dixon, S. F.; Tsuda, M. *Eur. Biophys. J.* **1986**, *13*, 195.

(23) (a) Bennett, N. *Biochem. Biophys. Res. Commun.* **1978**, *83*, 457. (b) Bennett, N. *Eur. J. Biochem.* **1980**, *111*, 99.

(24) Allan, A. E.; Cooper, A. *FEBS Lett.* **1980**, *119*, 238.



active site region (possibly introducing a negatively charged group into the vicinity of the Schiff base, with effects similar to those seen in the SDS model experiments), we have been unable to devise a rational scheme that satisfactorily accounts for the basic observations. An alternative explanation is that the retinal binding site changes relatively little, if at all, during recombination and that the adjacent positively charged group (lysine, arginine, etc.) responsible for depressing the reactive lysine  $pK$  in the apoprotein now actively participates in protonating the retinyl Schiff base nitrogen by formation of an  $(-NH\cdots N)^+$  hydrogen bond.<sup>19</sup> This clearly satisfies the requirement for no overall change in protonation during bleaching and regeneration of rhodopsin<sup>19</sup> (or bacteriorhodopsin<sup>28</sup>) at neutral pH, and is given theoretical support by recent *ab initio* calculations on protonated amine-imine hydrogen bonds.<sup>32</sup> In such circumstances the equilibrium position of the H-bond proton can depend critically on the relative orientations of the donor and acceptor groups and slight reorientations can result in the reversal of the relative  $pK$ 's of the groups involved, together with proton transfer from one nitrogen to the other. Such a process might form part of the proton translocation mechanism of bacteriorhodopsin<sup>32</sup> and also recalls the deuterium isotope effects observed in picosecond kinetic studies of rhodopsin photolysis which indicate proton translocation associated with formation of the primary batho intermediate.<sup>33</sup> Small changes in relative orientation during the primary *cis*-*trans* photoisomerization could result in translocation of the (exchangeable) proton within the  $NH\cdots N$  hydrogen bond. The red shift of bathorhodopsin with respect to the parent rhodopsin might indicate that proton transfer is toward the imine nitrogen in this case, implying that the Schiff base is only partially protonated in the unbleached pigment. Recent observations<sup>34</sup> on the effects of lysine methylation may be relevant here. Firstly, permethylation of all rhodopsin lysines, excluding the active lys-296, gives a spectrally identical protein which is fully viable as regards bleaching, regenerability, and biochemical activity. This permethylation converts the primary amino groups to tertiary dimethylamines, without loss of charge at physiological pH. If one of these lysines happened to be the putative adjacent group in the retinyl binding site, it would still be capable of  $NH\cdots N$  bonding and proton donation to the imine nitrogen, even in this modified form. A more interesting modification is that involving the additional monomethylation of lys-296 itself, which produces a bleachable pigment red shifted to about 520 nm.<sup>34</sup> In this case the methylated Schiff base nitrogen must carry the full formal positive charge and cannot H-bond to any adjacent group. Although there may be other explanations, the further red shift in this already anomalously bathochromic pigment suggests that only partial protonation is necessary to achieve the 500-nm  $\lambda_{max}$  of unmodified rhodopsin.

Regardless of the source of the perturbations, this reversal in  $pK$  of the active lysine and the chromophoric Schiff base has important consequences for the stability of the pigment under physiological conditions. The thermodynamic stability of model Schiff bases under normal conditions ( $K_{SH} > K_{BH}$ ) falls rapidly below the  $pK$  of the amine (see eq 2 and Figure 1), yet the rhodopsins are stable at neutral pH under conditions where model Schiff bases would hydrolyze rapidly. This is clearly not a simple kinetic stability due to protonation or inaccessibility to water since formation of the Schiff base (regeneration) is spontaneous under the same conditions. Reversal of the  $pK$ 's ( $K_{SH} < K_{BH}$ ) for whatever reason, however, reverses the situation such that thermodynamic stability is now greatest at low pH (eq 2). This,

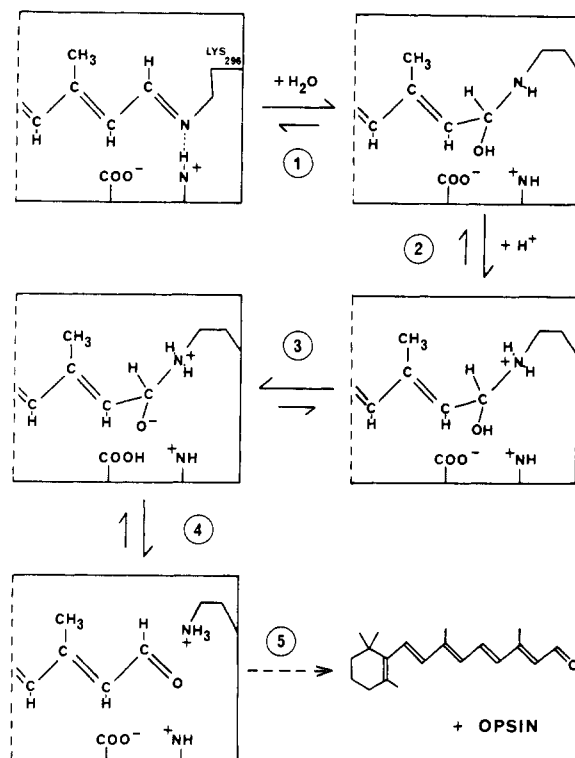


**Figure 10.** Outline scheme for the hydrolysis of the retinal Schiff base chromophore in the active site of rhodopsin, incorporating the tetrahedral carbinolamine intermediate, as a possible model for the Meta I-II transition (see text for details). Note that prior to release of the *all-trans*-retinal from the binding site (step 5), all steps are potentially reversible.

incidentally, is always the case for methylated Schiff bases where the permanently protonated imine becomes increasingly susceptible to hydrolysis by  $OH^-$  at high pH, and this may be of significance when considering the effect of such a modification on the meta-rhodopsin transition.<sup>34b</sup>

Other factors which must be taken into account when considering the possible retinal-opsin interactions include the electrical neutrality of the binding site<sup>35</sup> and the source of the chromophoric shift of rhodopsins. The most plausible explanations for the latter are various forms of the "point-charge" model,<sup>36</sup> which invoke the presence of a negatively charged carboxylate group close to the retinyl moiety in the active site (though positive groups may serve equally well). This is not inconsistent with our hypothesis of an additional positive group interaction with the imine nitrogen; indeed the pair may form a salt bridge and satisfy the electrical neutrality condition without requiring the presence of counterions in the retinal binding site. Furthermore, the conjugate base of an aspartic or glutamic acid residue close to the imine may serve an additional role in catalyzing hydrolysis of the Schiff base linkage at a later stage in photolysis (see below).

With the foregoing in mind, we can now begin to visualize a plausible sequence of events in the bleaching of rhodopsin. We imagine a rhodopsin binding site containing both an anion ( $-COO^-$ ) and a cation ( $-NH^+$ ) in close proximity to the 11-*cis*-retinal imine linkage. This linkage is (partially) protonated by  $(-NH\cdots N)^+$  bond formation to the adjacent cation. Initial photon absorption induces a rapid *cis*-*trans* isomerization of the retinyl group, and a slight reorientation in relative positions of the Schiff base and its adjacent H-bond donor reverses the relative  $pK$ 's of the two groups and forces translocation of the proton along the hydrogen bond toward the imine nitrogen to produce the red-

(32) (a) Hillenbrand, E. A.; Scheiner, S. *J. Am. Chem. Soc.* **1985**, *107*, 7690. (b) Scheiner, S.; Hillenbrand, E. A. *Proc. Natl. Acad. Sci. U.S.A.* **1985**, *82*, 2741. For similar suggestions concerning nonprotonated or H-bonded Schiff bases see, for example: (c) Favrot, J.; Leclerc, J. M.; Roberge, R.; Sandorfy, C.; Vocelle, D. *Chem. Phys. Lett.* **1978**, *53*, 433. (d) Rafferty, C. N.; Shichi, H. *Photochem. Photobiol.* **1981**, *33*, 229. (e) Merz, H.; Zundel, G. *Biochem. Biophys. Res. Commun.* **1986**, *138*, 819.

(33) Peters, K.; Applebury, M. L.; Rentzepis, P. M. *Proc. Natl. Acad. Sci. U.S.A.* **1977**, *74*, 3119.

(34) (a) Longstaff, C.; Rando, R. R. *Biochemistry* **1985**, *24*, 8137. (b) Longstaff, C.; Calhoon, R. D.; Rando, R. R. *Proc. Natl. Acad. Sci. U.S.A.* **1986**, *83*, 4209.

(35) Birge, R. R.; Murray, L. P.; Pierce, B. M.; Akita, H.; Balogh-Nair, V.; Finsden, L. A.; Nakanishi, K. *Proc. Natl. Acad. Sci. U.S.A.* **1985**, *82*, 4117.

(36) (a) Kropf, A.; Hubbard, R. *Ann. N.Y. Acad. Sci.* **1958**, *74*, 266. (b) Honig, B.; Dinur, U.; Nakanishi, K.; Balogh-Nair, V.; Gawinowicz, M. A.; Arnaboldi, M.; Motto, M. G. *J. Am. Chem. Soc.* **1979**, *101*, 7084. (c) Baasov, T.; Sheves, M. *Ibid.* **1985**, *107*, 7524 (see also ref 1e.)

shifted, more fully protonated bathorhodopsin intermediate. (This, incidentally, destabilizes the  $\text{NH}\cdots\text{N}$  bond<sup>32</sup> and may contribute in part to the large energy storage observed in this first step.<sup>22</sup>) On the picosecond scale of this process there is little time for any other major conformational changes, but subsequent structural relaxation in the immediate active site vicinity (to give lumirhodopsin) followed by more global conformational changes (giving metarhodopsin I) can be envisaged as the protein relaxes to accommodate the new retinal configuration. To our minds this exhausts the number of plausible conformational changes that may be invoked without the intervention of additional chemical processes, and by this stage the active site conformation has changed to a sufficient extent to reduce the stabilizing influences on the Schiff base linkage and to allow access to solvent water and the start of hydrolysis. A plausible mechanism for this stage is sketched in Figure 10. Attack of water, base catalyzed by the proximal point charge (glutamate or aspartate), forms the carbinolamine species (step 1). The consequent change from trigonal to tetrahedral configuration results in relative reorientation of active site contacts, breaking the  $\text{-NH}\cdots\text{N-}$  hydrogen bond and allowing conventional protonation (from the solvent) of the more basic carbinolamine (step 2). This is the proton uptake characteristic of the Meta I  $\rightarrow$  II transition.<sup>13</sup> Simple deprotonation of the carbinol by proton release to the solvent, required to form the zwitterionic species as the next stage of hydrolysis,<sup>2</sup> is inhibited by the adjacent carboxylate anion but could occur by proton transfer to this group (step 3), consistent with changes in carboxylate protonation revealed by FTIR difference spectra.<sup>37</sup> The linkage now finally breaks (step 4) to give the retinal aldehyde, held in place by noncovalent interactions. This noncovalent complex will be unstable, however, because of the sterically unfavorable trans configuration of the retinal and irreversible retinal dissociation can now take place (step 5), though this is not necessarily a straightforward process and could involve transimination

and transient, nonspecific Schiff base formation with adjacent amines along the way, giving a plausible explanation for the later metarhodopsin III and indicator-yellow intermediates.

There remain some paradoxes, however, and it is not clear at this stage which of the various species in Figure 10, following water attack on Meta I, are to be identified with the spectral Meta II state. The model compound stopped-flow experiments indicate that the retinal carbinolamine has spectroscopic properties similar to the parent Schiff base in detergent micelles, rather than the somewhat lower  $\lambda_{\text{max}}$  that might be anticipated by comparison with more stable pentaenes. It is difficult to predict the additional effects of point-charge interactions and possible chromophore strain during the metarhodopsin transition, but the 380-nm  $\lambda_{\text{max}}$  of Meta II is identical with that of free retinal and suggests the presence of the aldehyde at this stage. By contrast, the Raman spectrum of Meta II points more to some form of the carbinolamine. It seems feasible that the spectroscopically identified Meta II state is actually a dynamic mixture of the various chemical species that cannot be resolved in the UV/visible region, or which are sampled to differing extents by the different spectroscopic techniques. But, regardless of these uncertainties about the finer mechanistic details, we note that the significant change from trigonal to tetrahedral configuration at the retinal-opsin linkage during carbinolamine formation could be responsible, either directly or indirectly by inducing protein conformational changes, for triggering the G-protein activation and subsequent biochemical steps thought to be involved in the photoreceptor response and which have been shown to be initiated by the metarhodopsin II intermediate.<sup>34,38</sup>

**Acknowledgment.** We are grateful to Dr. S. W. Provencher for the provision of the DISCRETE program and to Professor L. D. Barron for advice and use of the Raman instrument. Financial support for equipment and research studentships (S.F.D. and J.L.R.) was from the U.K. Science and Engineering Research Council.

(37) (a) Siebert, F.; Mantele, W.; Gerwert, K. *Eur. J. Biochem.* **1983**, *136*, 119. (b) Rothschild, K. J.; Cantore, W. A.; Marrero, H. *Science* **1983**, *219*, 1333. (c) De Grip, W. J.; Gillespie, J.; Rothschild, K. J. *Biochim. Biophys. Acta* **1985**, *809*, 97.

(38) (a) Bennett, N.; Michel-Villaz, M.; Kuhn, H. *Eur. J. Biochem.* **1982**, *127*, 97. (b) Emeis, D.; Kuhn, H.; Reichart, J.; Hofmann, K. P. *FEBS Lett.* **1982**, *143*, 29.

## Deuterium Isotope Effects on the Carbon-13 Chemical Shifts in 2-Substituted 2-Norbornyl Cations

Kenneth L. Servis,\*<sup>1a</sup> Robert L. Domenick,<sup>1a</sup> David A. Forsyth,\*<sup>1b</sup> and Yi Pan<sup>1b</sup>

Contribution from the Department of Chemistry, University of Southern California, Los Angeles, California 90089, and the Department of Chemistry, Northeastern University, Boston, Massachusetts 02115. Received October 31, 1986

**Abstract:** Deuterium isotope effects on  $^{13}\text{C}$  chemical shifts have been examined as a function of location of deuterium in the  $\text{C}_3$ -exo or  $\text{C}_3$ -endo positions and as a function of increasing electron demand in the series 2-norbornanone, 2-aryl-2-norbornyl cations, and 2-methyl-2-norbornyl cation. Comparison with isotope shifts in 2-aryl-2-propyl cations demonstrates a change in the type of response to isotopic perturbation in 2-aryl-2-norbornyl cations as electron demand increases. The results are consistent with the onset of  $\sigma$ -bridging as electron demand increases. The observed isotope shift at a cation center is suggested to be a sum of contributions from a small upfield shift due to perturbation of the  $\sigma$ -framework (inductive-type perturbation), a downfield shift due to perturbation of hyperconjugation, and a potentially large upfield shift from perturbation of three-center, two-electron bonding. NMR isotope shifts may be a particularly sensitive probe of  $\sigma$ -bridging because of the vibrational origin of the isotope effect.

We present here deuterium isotope effects on the  $^{13}\text{C}$  chemical shifts of several 2-substituted 2-norbornyl cations and related compounds. The variation of NMR isotope shifts as a function of aryl substituents in 2-aryl-2-norbornyl cations is examined with the aim of detecting bonding changes that may occur with increasing electron demand. The results are analyzed in terms of

possible mechanisms of isotopic perturbation of the vibrationally averaged structure that could lead to the observed effects on shielding.

Substitution for hydrogen by deuterium produces small but measurable changes in  $^{13}\text{C}$  NMR chemical shifts.<sup>2-4</sup> Intrinsic

(1) (a) University of Southern California. (b) Northeastern University.

(2) Batiz-Hernandez, H.; Bernheim, R. A. *Prog. NMR Spectrosc.* **1967**, *3*, 63.